

Towards the understanding of the interfacial pH scale at Pt(111) electrodes.

Rubén Rizo^{1,2}, Elton Sitta^{1,3}, Enrique Herrero^{1*}, Víctor Climent^{1*}, Juan M. Feliu¹

(1) *Instituto de Electroquímica, Universidad de Alicante, Apdo. 99, E-03080 Alicante. Spain.*

(2) *Present address: Departamento de Química Física, Universidad de La Laguna,*

Astrofísico F. Sánchez s/n, 38071 La Laguna, Tenerife, Spain

(3) *Present address: Universidade Federal de São Carlos, Departamento de Química,*

Rodovia Washington Luiz, Km 235, Caixa Postal 676 CEP 13565-905, São Carlos, SP, Brasil

* emails: herrero@ua.es, victor.climent@ua.es

Key words

Pt(111); pztc; pzfc; interfacial pH

Abstract.

The determination of the potentials of zero total and free charge, pztc and pzfc respectively, were made in a wide pH range by using the CO displacement method and the same calculation assumptions used previously for Pt(111) electrodes in contact with non-specifically adsorbing anions. Calculation of the pzfc involves, in occasions, long extrapolations that lead us to the introduction of the concept of potential of zero extrapolated charge (pzec). It was observed that the pztc changes with pH but the pzec is independent of this parameter. It was observed that the $pztc > pzec$ at $pH > 3.4$ but the opposite is true for $pH < 3.4$. At the latter pH both pzec and pztc coincide. This defines two different pH regions and means that adsorbed hydrogen has to be corrected in the “acidic” solutions at the pztc while adsorbed OH is the species to be corrected in the “alkaline” range. The comparison of the overall picture suggests that neutral conditions at the interface are attained at significantly acidic solutions than those at the bulk.

Introduction.

The importance of the charge has been often emphasized as one of the relevant electrical variables, in addition to the potential, that determines the properties of the electrified interface. Charge, and not only the potential, will have large implications in the overall electrochemical reactivity of a particular system. Ionic and molecular adsorption, as well as dipole orientation, depends on the sign and magnitude of the charge separation at the interphase. Electrocatalytic reactions always proceeds through adsorption steps that will either be directly sensitive to the charge or indirectly sensitive through the competition with other adsorbed species or even with the adsorbed water. To establish the unambiguous relationship between electrode potential, which is the directly measurable quantity, and the interfacial charge, knowledge of the potential of zero charge (pzc) is necessary.

Different methodologies have been developed for the determination of the pzc of different metals [1-5]. Historically, most of the theories of interfacial electrochemistry were developed for mercury electrodes, where pzc measurements can be easily achieved from electrocapillary curves [6]. Studies with solid electrodes were delayed by the existence of intrinsic difficulties associated with these measurements. First, heterogeneities on the surface greatly complicate the interpretation of the result and make necessary the use of single crystal surfaces. Secondly, accumulation of impurities on the surface of the electrode could strongly affect the structure of the double layer and therefore imposes the use of ultrapure solutions and the development of suitable methods for the cleaning of the electrode surface without affecting its atomic structure [7]. One iconic moment in the development of interfacial electrochemistry with solid metals is the introduction by Jean Clavilier of the flame annealing methodology [8, 9]. This methodology has been successfully extended for gold, platinum, rhodium, iridium, palladium and even silver electrodes [10].

Measurement of interfacial tension of solid electrodes is challenging [11-15] and alternative methods are necessary for the determination of pzc. In the absence of specific adsorption, that is, when Gouy Chapman Stern theory is satisfied, the pzc can be determined from the location of the minimum in the differential capacity in diluted solutions, as predicted by this theory. This method has been successfully applied to other electrodes, particularly to gold and silver fcc metals, for which it has been often demonstrated the significant effect of surface structure on interfacial parameters, in particular on the pzc [16]. In the case of gold, particular care should be taken to control the nature of the surface structure since this can be easily altered by the surface reconstruction phenomena [7, 17]. For gold and silver, a lot of information has been gathered about the influence of the surface structure [17-21], specific adsorption and temperature [22-27] on the potential of zero charge.

The scale of electrode potentials has often been related to work function measurements. The latter can also be understood as a measure of the potential difference between a metal and a vacuum reference system. The relationship between both magnitudes has often been discussed [2, 28-30]. This relationship should take into account the influence of the solvent on the surface potential of the metal (spillover of electrons) and the dipolar contribution to the surface potential as well as the electrostatic potential created by the separation of charges at the interface. The correct comparison between electrode potential and work function should be done in the absence of charge, i.e. at the pzc. Ionic or dipolar adsorption at the pzc will also compromise the comparison with the work function and, therefore, any comparison between pzc and work function should take into account the particular composition of the electrochemical interphase. Given the relationship between these two properties, it is possible to employ all the knowledge available in the understanding of work function measurements to explain trends in the pzc in electrochemical environment. This is the case of the variation of pzc in stepped surfaces with the step density that has been

explained in terms of Smoluchowski effect[18]. This implies the appearance of surface dipoles associated to step sites due to the spillover of electrons from the top to the bottom part of the step.

The determination of the pzc in the presence of electrosorption processes is less straightforward. This is the case of metals that adsorb hydrogen, like platinum, palladium, rhodium and iridium, which are, indeed, the most electrocatalytic materials. It is also the case of gold or silver electrodes in the presence of a metal upd process or when the electrode surface is covered with a thiol monolayer [31]. First, the identification of the minimum in the differential capacity is precluded by the overlapping of the pseudocapacity phenomena [32]. Secondly, the meaning itself of the concept of charge is obscured by the interference of adsorption processes that involve charge transfer [3, 4]. In this regards, it turns out that it is not possible to unambiguously discriminate only from macroscopic electrochemical measurements whether there is a true charge separation at the interface (true capacitive charge) from a situation where charge has been redistributed to form covalent bonds between the surface and the adsorbed species (pseudocapacity phenomena). In this regards, it is necessary to distinguish between the concepts of free charge (the true electronic excess charge on the metal balanced by ionic charge in the electrolyte) from the concept of total charge, which includes all the charge that flows through the external electric circuit, that is, both the capacitive and the faradaic charge. An alternative definition of free and total charge were given in reference [31] where free charge is called charge at a constant surface coverage. However, in the present paper, we prefer to keep the terminology free and total charge. Consequently with these definitions there will be two different values of pzc, the potential of zero free charge, pzfc, and the potential of zero total charge, pztc. The first one is that related with the structural microscopic properties of the interface, such as work function, dipole orientation, etc. and is equivalent to the pzc in non-hydrogen adsorbing metals (also to the

potential of zero charge at constant adsorbed species). However, the latter is the only one accessible from electrochemical measurements. Calculation of the pzfc from pztc (or other macroscopic measurements) always involves additional (extrathermodynamic) assumptions. Alternatively, the position of the pzfc can be inferred from indirect measurements, like the reorientation of water dipoles as monitored with infrared spectroscopy [33] or laser induced temperature jump measurements [34-41]. It is also worth mentioning in this context the studies in UHV of model double layer systems created by sequential dosing of the same components of the true double layer in electrochemical environment [42, 43]. This involves water dosage together with alkali metals to simulate the presence of ions. Work function measurements of such synthetic double layer structures leads to an indirect estimation of the pzfc. This calculation involves the use of an estimated value of the reference electrode potential, which is subject to some uncertainty.

In this paper, an extension of the measurements to alkaline solutions is attempted. In the following section the general strategy to measure the pzfc will be described in such a way that the whole methodology could be used in acidic and alkaline solutions.

1.1.Charge evaluation

The determination of the total charge on platinum electrodes can be achieved with the CO charge displacement experiment. In this experiment, CO is introduced in the atmosphere of the electrochemical cell, while the electrode is polarised at a constant potential. Adsorption of CO causes the flowing of charge through the external circuit to maintain the imposed potential value. The magnitude of the charge flowing is equal to the difference between the interfacial charge on the CO covered electrode and the charge present at the beginning:

$$q_{disp.} = q_{CO} - q(E) \quad (1)$$

To proceed with the analysis of the data, it was initially assumed that the charge on the CO covered electrode, q_{CO} , is negligible [44]. This assumption was based on the very low differential capacity that can be measured for this interphase. With this assumption it was concluded that the displaced charge is equal in magnitude but with opposite sign, to the charge at the interphase at the potential of the experiment. This assumption was later refined from an estimation of the value of the pzc of the CO covered surface, inferred from UHV measurements for the Pt(111)-CO surface [43]. With this information q_{CO} can be calculated according to:

$$q_{CO} = \int_{pzc}^E C_{CO} dE \quad (2)$$

Where C_{CO} is the differential capacity of the CO covered interphase. Considering that, according to this estimation, the pzc of the CO covered surface is around 1.0 V (SHE) and that the differential capacity is around $14 \mu\text{Fcm}^{-2}$, a residual charge, $q_{CO} = -14 \mu\text{Ccm}^{-2}$ at 0.03 V (SHE), can be calculated. Indeed, this charge represent a small contribution to the total displaced charge, q_{dis} , but has an important effect on the further treatment of the data for the calculation of the pzc as discussed below. More recently, the charge q_{CO} has been measured for Pt(111) in acid solutions by recording the transients currents that take place after contacting the dry CO-covered surface with the electrolyte at constant potential [45]. Extreme precautions have to be taken during these measurements to avoid the formation of a double layer prior to the contact of the electrode with the electrolyte, as could be caused by the presence of charge transfer processes like oxygen reduction. The results obtained with this measurements were consistent with the estimation previously discussed.

As concluded from the previous paragraphs, the CO charge displacement provides the total charge at the potential of the measurement. Therefore, to locate the pzc, charge displacement experiments should be repeated at different potentials, or alternatively, the

measurement at just one potential can be combined with the integration of the voltammetric currents to calculate the charge vs potential curve according to:

$$q(E) = q(E^*) + \int_{E^*}^E \frac{j}{\nu} dE \quad (3)$$

where E^* is the potential of the charge displacement experiment, $q(E^*)$ can be obtained from this experiment, through a combination of equations (1) and (2), j is the voltammetric current and ν is the sweep rate. Figure 1 illustrates this procedure for the case of Pt(111) in 0.1 M HClO₄. The voltammogram here exhibits the well-known features for a well ordered Pt(111) surface in this electrolyte. In particular, voltammetric currents below 0.3 V (SHE) correspond to hydrogen adsorption/desorption to achieve a maximum coverage of 0.67 monolayers, while currents above 0.53 V (SHE) correspond to hydroxyl adsorption/desorption up to a coverage of ca. 0.5. Both regions are separated by the so called double layer region characterized by relatively low current values (equivalent to a capacitance of ca. 65 μFcm^{-2}). The absence of peaks at 0.05 and 0.19 V, that would indicate the presence of (110) and (100) defects, is a clear indication of the good quality of the electrode employed in this study. Integration of the voltammetric charge using equation (3) with $E^* = 0.03$ V and $q_{CO}(0.03 \text{ V}) = 141 \mu\text{C cm}^{-2}$ provides curve b). Once the curve $q(E)$ has been obtained, the pztc can be directly measured from the intersection of this curve with the axis of abscissas. The result shown in figure 1 intercepts the axis at ca. 0.27 V, value that can be taken as a first approximation to the pztc. This value can be refined with the consideration of q_{CO} , as discussed above. Because q_{CO} is negative, this correction displaces the $q(E)$ to lower values, resulting in curve c) in figure 1. With this correction, the pztc shifts to 0.32 V, that is, the effect of neglecting q_{CO} induces an error of ca. 50 mV in the pztc. Charge curves obtained as discussed in this paragraph are very important to understand the electrochemistry of platinum. They allow the discrimination of hydrogen and anion adsorption from the sign of the charge at each potential. They are also of

great value for double layer corrections in coulometric measurements through stripping experiments, since after stripping an adlayer, the total charge of the free surface should be recovered, as given by the $q(E)$ curve. This charge needs to be taken into account for the correct calculation of the coverage from the stripping charge [46].

While the pztc values obtained from CO displacement are only subject to the uncertainty in the estimation of the pzc of the CO covered electrode, much more difficult is the calculation of the pzfc. Values of pzfc has been estimated for Pt(111) and vicinal surfaces under the assumption that only free charge is present on the interphase in the so called double layer region, between 0.33 and 0.53 V. This assumption is reinforced by the variation of the total charge curves with the pH in this potential region: while all features associated with hydrogen and OH adsorption are expected to shift with pH, free charge is expected to be independent of pH [47]. With this assumption, if total and free charges are equal in the double layer region and if pztc fell in this region, pztc and pzfc would also coincide. In acid solution for Pt(111) and vicinal surfaces, pztc lies at the beginning of the hydrogen adsorption region, as shown in figure 1 and further calculation are necessary for the estimation of the pzfc. Knowledge of the free charge at one given potential could be combined with double layer capacity to obtain the curve corresponding to free charge in a way completely analogous to equation (3):

$$\sigma(E) = \sigma(E^*) + \int_{E^*}^E C_{dl} dE \quad (4)$$

where $\sigma(E)$ is the free charge and $\sigma(E^*)$ can be obtained from the curve $q(E)$ in the region between adsorption of hydrogen and OH ions where the condition $q(E^*) = \sigma(E^*)$ is satisfied, and C_{dl} is the differential capacity corresponding only to truly capacitive processes:

$$C_{dl} = \left(\frac{\partial q}{\partial E} \right)_{P,T,\mu_i,\Gamma_i} = \left(\frac{\partial \sigma}{\partial E} \right)_{P,T,\mu_i,\Gamma_i} \quad (5)$$

This calculation would require knowledge of C_{dl} which is a magnitude usually not available. C_{dl} has been obtained for Pt(111) from the analysis of the charge curves as a function of pH through a thermodynamic method that involved some extrathermodynamic assumptions [47]. It was shown that C_{dl} has a maximum around the value of the pzfc and then decreases to ca. $15 \mu\text{Fcm}^{-2}$. This value of double layer capacitance is consistent with impedance measurements of this magnitude [48, 49]. With this information it could be concluded that pzfc and pztc almost coincided in the case of Pt(111) with a value of 0.32 V SHE. This value agrees reasonable well with the position where water dipole reorientation is inferred from IR measurements [33] and laser induced temperature jump experiments [34, 40]. A maximum in the differential capacity has been indeed interpreted as a consequence of dipole reorientation [32], although in this case, it was proposed that the pzfc does not coincide with the peak but it is located at higher potentials, in the OH adsorption region. This assumption was based on the absence of the minimum in the differential capacity in diluted solutions predicted by Gouy-Chapman theory. However, the location of the pzfc in the OH adsorption region would imply that OH adsorption starts within the hydrogen region, what is contradiction with the thermodynamic analysis reported in [47]. The reason for the absence of a minimum in the differential capacity is unclear at this point.

When knowledge of C_{dl} is not available, still a rough estimation of the location of the pzfc can be obtained by considering a value of C_{dl} approximately constant and equal to its value in the double layer region ($65 \mu\text{Fcm}^{-2}$ in this case). This is equivalent to perform a linear extrapolation of the charge $\sigma(E)$ from the double layer into the hydrogen (or OH, for alkaline pH values) region as shown by line d) in figure 1. In this way, a value of potential of zero extrapolated charge (pzec) around 0.28 V(SHE) is obtained, slightly lower than the value

reported before using the thermodynamic calculation of C_{dl} . With the assumption of a constant C_{dl} , values of p_zec for Pt(111) vicinal surfaces were obtained as a function of the step density [50]. In this case, the p_zec decrease as the step density increases with a slope similar to that described by the variation of the work function. While the extrapolation of the free charge into the hydrogen (or hydroxyl) adsorption region is not absent from some uncertainty, it is expected to provide valid values of p_zfc for short extrapolation ranges. As the thermodynamic method used to calculate C_{dl} cannot be used in alkaline solutions we will maintain this simpler correction to separate total and free charge in the analysis presented in this work. In some cases, the extrapolation involves a longer range of potential values. In this case, the p_zec is likely to be different from the p_zfc. Still, the method can be valid to predict trends in the effect of pH in this important magnitude.

2. Experimental

The experiments were performed in a classical three electrode cell with two compartments. One of the problems working in alkaline solutions is the stability of the cell material in the time required for the experiment. Glass cells are more convenient since allow easier visualization of the meniscus, but possible glass corrosion can take place in alkaline solutions. Glass corrosion often causes contamination of the solution as clearly appears in some cases as reflected in progressive changes in the voltammogram from the characteristic behavior in clean solutions [51], with the progressive increase of a new peak at ca. 0.5 V RHE. Several causes are considered to be at the origin of this problem, yet observed many years ago and attributed to sulfate contamination [51] but more likely this effect is due to the presence of iron group metals [52]. In our case, we have also identified iron by XPS on electrodes in which the impurity has extensively accumulated.

To check the origin of this problem we have used Teflon cells and also a platinum crucible as the cell body, inside a glass vessel filled with Ar. The platinum crucible can be flame annealed immediately before use, resulting in the cleanest possible container. On the other hand, some pre-electrolysis experiments were attempted to improve the purity of the solution. It was concluded that, if impurities are present in the solution, the voltammograms showed their contribution (peak at 0.5-V RHE) independently of the material used as cell body. The preelectrolysis may help to remove significant fractions of the contamination in this case. It was also concluded that a source of NaOH usually behaves properly after opening the fresh new product, but start degrading after some days of working. This clearly points to a degradation coming from dust impurities. In this respect, if one wants to work under well-defined conditions, freshly open flasks should be used and, as always, fresh solutions should be prepared every day, storage is not recommended in any case. With these precautions it is possible to work with glass cells without appreciable contamination in the time scale of the experiments presented in this work. Other important precaution is to purge the Ar gas lines in order to avoid self-contamination while deoxygenating the solution.

Another point deals with the evaluation of the charge remaining at the surface covered by CO. The determination of the capacitive currents in alkaline solutions are difficult because the permanent presence of the prewave oxidation at low potentials, probably due to a defective CO adlayer [53]. However, it was possible to perform this calculation by careful control of the potential range. This procedure leads to reliable results as it will be described in the next section.

Working electrodes were platinum single crystals with (111) surface orientation and were prepared from small beads, ca. 2 mm in diameter, obtained by the method described by Clavilier et al. [54]. Prior to any experiment the working electrodes were flame annealed in a propane-oxygen flame, cooled in a hydrogen/argon (1:4) atmosphere and transferred to the

cell protected by a drop of ultra-pure water saturated with these gases. Solutions were prepared by using NaOH (Aldrich, twice distilled or Merck suprapur), suprapur grade sodium carbonate and bicarbonate (Aldrich), concentrated perchloric acid (Merck Suprapur), and ultrapure water from Elga Purelab Ultra Analytic system (Resistivity 18.2 M Ω cm). H₂, CO and Ar were also employed (N50, Air Liquide). Voltammetric curves were recorded with a signal generator (PAR 173), a potentiostat (Edaq EA161) and a digital recorder (eDAQ, ED401). Curves were obtained in a hanging meniscus electrode configuration. The stability of the voltammetric profiles was carefully checked to ensure solution cleanliness and surface order. All potentials have been measured using a reversible hydrogen electrode (RHE) and transformed to the SHE when required. After each experiment the solution pH was calculated, in all cases, by the measuring the potential difference between the corresponding RHE and a Ag/AgCl reference electrode by using a electrochemical analyzer (μ Autolab type III). The electrolyte composition and pH data of all the solutions employed in this work are given in table 1. Also, figure 2 shows the voltammetric profiles of the Pt(111) electrode in the different electrolytes plotted in the SHE scale.

CO displacement experiences were performed by following the same methodology employed before in our research group [44]. The experiment was performed on well characterized electrodes and consist in the following steps: i) A 0.1V constant potential was fixed, which is maintained during the CO displacement experience. A suitable flow of CO was introduced in the electrochemical cell while the transients current, produced in response to the introduction of this gas, was registered; ii) When current decays to zero, indicating surface saturation, the CO flow was stopped and the excess CO in the solution and the cell atmosphere was removed by bubbling argon during 7-10 minutes; iii) the surface blockage was checked in the low potential range previously to the stripping of the CO monolayer, in a single sweep; iv) the recovery of the initial surface profile is then verified. The experiments

were repeated again several times, starting in each case from flame annealed electrodes, to ensure reproducibility. The series of experiments were repeated at least three different days.

One important aspect is to ensure the absence of faradaic currents overlapped with CO displacement currents. In this sense is important to minimize the possible contribution due to traces of oxygen presents in the cell atmosphere. More important is to prevent the entry of oxygen together with the flow of CO into the cell. So the inlet conduction of CO must be entirely purged with argon before each experiments. A side outlet in the CO conduction ensures a continuous flow of CO, preventing that possible traces of oxygen, which could enter by effusion through the walls of the tube, and then could be accumulated. In addition, nylon tubes were employed in the experimental set-up in order to ensure good oxygen impermeability.

3. Results

3.1. Acidic solutions (pztc > pzec)

Experiments like that reported in figure 1 were performed for solutions of different pH in the present study. By using a simple extrapolation of the double layer region a pzec of 0.28 V vs SHE was calculated for this figure (pH=1.2). This value is slightly lower (ca. 40 mV) than that calculated after evaluation of the C_{dl} in previous studies [47], but within the error of the measurements than that calculated using a linear extrapolation of the double layer [50]. The difference can be due to the different data treatment and could also reflect the experimental uncertainty coming from the CO dosing and subsequent charge displacement experiment. The voltammetric features due to hydrogen and hydroxyl adsorption shift with pH ca. -60 mV/decade, as expected from Nernst equation. If pztc were strongly influenced by these processes, it should shift accordingly. This is the case of Pt(110) and Pt(100) [40]. However, when the pztc lies close or within the double layer region, less influence from

these adsorption processes is expected and the shift of pztc with pH should be smaller or there should be no shift at all. Figure 3 shows the particular example of pH = 3.4. At this pH the CO displaced charge at 0.1 V (RHE) amounts to $140 \mu\text{C cm}^{-2}$. Consequently, the uncorrected charge/potential curve would lead to a pztc of 0.16 V (SHE) and the pzec would be 0.08 V (SHE) (table 2). After correction of the remaining charge in the CO covered surface, q_{CO} , the curve is shifted towards lower charge values and the pztc is exactly zero at 0.28 V(SHE), coinciding with the same value reported above for pH=1.2 (figure 1). Unlike more acidic solutions, the pztc lies in the double layer region and there is no adsorbed hydrogen charge that had to be compensated ($q = \sigma$). Then, at these conditions it is not required any further estimation of C_{dl} to determine the pzfc. In fact, in this particular pH, both pztc and pzfc coincide without necessity of further refinements.

In this way, the pzfc appears to be a constant value in acidic perchloric acid solutions of different pH. The pztc values of the corrected charge curves shift to lower potentials in the SHE scale, but then pzfc is the same in all cases. It is not convenient to further increase the pH in this range, because the reversibility of the hydrogen adsorption region is not good enough in unbuffered solutions [55] and the charge density measurement would be unreliable. Instead it is more convenient to shift to alkaline solutions.

3.2. Alkaline solutions (pztc < pzec)

In order to estimate the double layer current at the Pt(111) surface covered by CO, as done in acidic solutions, the problem that appears is the interference of the CO oxidation prewave, which is much more noticeable in alkaline than in acidic solutions, and leads to unusually large values of the double layer. In this respect the strategy used was that described previously[53]: in separate experiments, the CO was dosed in acidic solution and then transferred to alkaline solutions of different pH. This leads to a slightly better ordered layers

in which the prewave is not observed [53]. The double layer capacity of the CO covered electrode increases with pH (Figure 4) and the corrections were performed accordingly. In any case, it should be stated that the differences in charge at the pztc after using different values are small and in all cases, the extrapolated values led to the same p_zec within the experimental error.

Figure 4 reports some voltammetric profiles in two alkaline solutions. In panel A the solution pH is 8.4 and the CO displaced charges at 0.1 V (RHE) amount to 136 $\mu\text{C cm}^{-2}$. Consequently the pztc on the uncorrected current density/potential curve is -0.122 V (SHE). After correction, curves shift to lower charge density values and the pztc is now 0.120 V (SHE), i.e. in the OH adsorption region. The same happens at pH 12.3 (Figure 5 panel B): the displaced CO charge at 0.1 V in the RHE scale amounts to 129 $\mu\text{C.cm}^{-2}$. This leads to an uncorrected pztc of -0.326 V (SHE). After correction of the CO remaining charge, all the curve shifts to negative charge values and the pztc shifts to -0.049 V (SHE), again at the beginning of the usual OH adsorption region. If we correct the OH adsorption charges at both pztc's by using the same procedure, that is, extrapolating the linear segment of the charge density/potential curve in the double layer region, we will get a p_zec higher than the pztc. Again, the value of the p_zec extrapolated in the corrected charge density/potential curves at both pHs is 0.28 V (SHE). Previous results with polycrystalline Pt and Rh samples in smaller pH range showed some dependence of the p_zfc with the pH [56]. The difference with the observed behavior reported here for the Pt(111) electrode may arise from the different behavior of adsorbed OH and H with de pH depending on the surface structure.

As remarked before, it should be kept in mind that the long extrapolation of the free charge introduces significant uncertainty in the final value of the p_zec. For this reason, we have chosen here to call this parameter p_zec and not simply p_zfc, to stress that both properties are most likely different. However, trends derived from the p_zec are a good indication for the

expected trends of the true pzfc values. In this regard, comparing acid and alkaline solutions, a clear trend is revealed despite the uncertainty introduced by the extrapolation: because the voltammetric profiles have shifted to negative potentials in the SHE scale the corrected charges in the double layer region are now negative. This creates a different situation than in the preceding section, because the extrapolation of the linear part of the corrected charges should be performed towards more positive potentials, resulting a pzec higher than the pztc. This can be easily done as exemplified in figure 5 for two pH values. Interestingly, the pzec values coincide in both alkaline and acid solution with the value given above: 0.28 V.

4. Discussion

The experimental results can be summarized in Table 2, but the most relevant points can be seen in Figure 6. There are two main features: first of all, the pzec is 0.28 V (SHE), independent of pH. The pztc's at different pH's correspond to different surface compositions, in acid solutions the surface contains adsorbed hydrogen while in alkaline solutions the surface contains adsorbed OH. The total charge is defined as:

$$q = \sigma - F\Gamma_H + F\Gamma_{OH} \quad (6)$$

In acidic solutions, the pztc lies in the hydrogen region and

$$\sigma = F\Gamma_H \quad (q = 0) \quad (7)$$

Therefore, the extrapolation is to lower potential until this positive value of free charge is cancelled. In alkaline solutions, the pztc lies in the hydroxyl region and

$$\sigma = -F\Gamma_{OH} \quad (q = 0) \quad (8)$$

Therefore, the free charge at the pztc is negative and the extrapolation has to be to more positive potentials. The curve at which both pzfc and pztc are the same, and indeed the charge density vanish is obtained to pH=3.4. This zero charge potential and this particular pH value can be considered as an intrinsic property of the Pt(111) electrode.

The situation at $\text{pH}=3.4$ defines two regions in which the pseudocapacitive contribution should be corrected: in acidic solutions the metal at zero total charge contains a small amount of adsorbed hydrogen and the solution side is acidic; in alkaline solutions the metal contains a small amount of adsorbed OH and the solution is alkaline. We can accept that at $\text{pH} = 3.4$ the metal side of the interface is pure platinum and the solution side is equilibrated from the neutrality viewpoint. This means that the solution does not contain any excess of positive or negative ions and thus would correspond to the conditions that define neutral solution. In this respect, the interfacial neutral pH would be 3.4, lower than the familiar 7 value in bulk solution.

The second point is that the extrapolation required to calculate the pzc define straight lines with slightly different slopes, depending on the solution pH. At $\text{pH}>3.4$, the slopes in the double layer region are smaller than those measured in the acidic region. This effect can be observed by comparing the voltammetry in the different media. As figure 2 shows, the currents in the double layer regions are higher in acid solutions, when compared to those recorded in alkaline solutions. This leads to charge curves in acidic solutions that are steeper than those recorded in alkaline solutions. A similar, but opposite, change in the differential capacity is reported in Figure 4 for the CO covered electrode, which also reflects a change in the double layer properties as the pH changes. This different slope could also reflect the different composition of the solution side of the interface which contains water and protons in “acidic” solutions and water and hydroxyls in “alkaline” solutions.

The difference in the acid-base behavior at the interface as compared to the solution has been found in previous studies dealing with anion adsorption. It was observed that CO_2 adsorbs as carbonate or bicarbonate at the surface of Pt(111) despite of the fact that the acidity constants predict that there is not any of these species in the bulk solution [57]. In a similar way, the adsorbate in sulfuric acid solutions has been demonstrated to be sulfate,

finishing a long polemic in the literature [58, 59]. It appears that the pK_a of acids is lower when adsorbed at the surface than in bulk solution. This is most likely related to the electron density withdrawal effect of the bond with the metal surface. Water may be considered as an acid or as a base and it is not strange that should follow similar trends. In fact, pure water surfaces are considered to be acidic with a $pH < 4.8$ due to site preference of protons at the surface [60, 61].

5. Conclusions.

In this manuscript, the $pztc$ and $pzfc$ have been calculated both in acidic and alkaline solutions. For the determination of the $pzfc$, a linear approximation for the charge in the double layer has been used, resulting into values of potential of zero extrapolated charge, $pzec$. As expected, it has been found that the $pzec$ is pH independent and it is located at 0.28 V (SHE). Although the treatment used here is less accurate than that used in acidic solutions, in which the C_{dl} contribution can be calculated, the conclusions are similar: the $pzfc$ is 0.28 V SHE while the $pztc$ changes with pH [47]. In the present approach, the remaining charges at the $pztc$ are reasonably small and define a constant $pzec$, 0.28 V SHE, which reasonably agrees with that calculated in the rigorous treatment. In turn, the less strict approach used here enables the calculation of the $pzec$ in alkaline solutions. Interestingly, data show that all $pzec$'s agree around a similar value, either with those calculated in acid solution and provides the conclusion that the neutrality condition is reached at pH 3.4 at the surface of Pt(111) electrodes.

Clearly more work should be made to confirm these conclusions, notably involving bulk alkaline solutions in which it would be desirable to define experimental conditions enabling to evaluate C_{dl} at different potentials, as done in acidic solutions. This would require finding an adsorbate [47] having the same features as chloride in acidic solutions of different

pH. Other options are also possible and the results from the laser temperature jump method, which provide the potential of maximum entropy in the double layer formation, μ_{me} closely related to the μ_{zfc} , are being currently examined.

Acknowledgements

Support from MINECO (Spain) through project CTQ2013-44083-P is greatly acknowledged. E.S. also thanks CNPq (Brazil) for the scholarship (grant No. 200939/2012-2).

References

Table 1. Electrolyte composition and corresponding pH of the solutions employed.

Electrolyte composition.	pH
0.1 M NaOH	13,1
0.09 M KClO ₄ +0.01 M NaOH	12,3
0.099 M KClO ₄ +0.001 M NaOH	11,1
0.1 M NaHCO ₃	8,4
0.099 M KClO ₄ +0.001 M HClO ₄	3,4
0.09 M KClO ₄ +0.01 M HClO ₄	2,32
0.1 M HClO ₄	1,2

Table 2. Values of the pztc and pzfc for the different solutions

pH	RHE scale				SHE scale			
	pztc uncorrected	pztc corrected	pzfc uncorrected	pzfc corrected	pztc uncorrected	pztc corrected	pzfc uncorrected	pzfc corrected
13,1	0,462	0,699	0,458	1,054	-0,313	-0,076	-0,317	0,279
12,3	0,406	0,679	0,406	1,013	-0,326	-0,049	-0,326	0,285
11,1	0,408	0,685	0,443	0,941	-0,249	0,028	-0,214	0,284
8,4	0,375	0,617	0,325	0,779	-0,120	0,122	-0,170	0,282
3,4	0,363	0,483	0,284	0,483	0,162	0,282	0,083	0,282
2,32	0,348	0,436	0,227	0,422	0,211	0,299	0,090	0,285
1,2	0,338	0,389	0,160	0,343	0,267	0,318	0,089	0,272

[1] J.O.M. Bockris, S.D. Argade, E. Gileadi, *Electrochim. Acta*, 14 (1969) 1259-1283.

[2] S. Trasatti, E. Lust, *The potential of zero charge*, in, Kluwer Academic/Plenum Publishers, New York, 1999, pp. 1-215.

[3] A.N. Frumkin, O.A. Petrii, *Electrochim. Acta*, 20 (1975) 347-359.

[4] A.N. Frumkin, O.A. Petrii, B.B. Damaskin, *Potential of Zero Charge*, in, Plenum, New York, 1980, pp. 221-289.

[5] O.A. Petrii, *Russ. J. Electrochem.*, 49 (2013) 401-422.

[6] D.C. Grahame, *Chem. Rev.*, 41 (1947) 441-501.

[7] A. Hamelin, *J. Electroanal. Chem.*, 407 (1996) 1-11.

[8] J. Clavilier, *J. Electroanal. Chem.*, 107 (1980) 211-216.

[9] J. Clavilier, R. Faure, G. Guinet, R. Durand, *J. Electroanal. Chem.*, 107 (1980) 205-209.

[10] J. Clavilier, *Flame-Annealing and Cleaning Technique*, in: A. Wieckowski (Ed.) *Interfacial Electrochemistry*, Marcel Dekker, Inc., New York, 1999, pp. 231-248.

[11] A.Y. Gokhshtein, *Electrochim. Acta*, 15 (1970) 219-223.

[12] G. Valincius, *Langmuir*, 14 (1998) 6307-6319.

- [13] R. Raiteri, H.J. Butt, *J. Phys. Chem.*, 99 (1995) 15728-15732.
- [14] J.H. Chen, L.H. Nie, S.Z. Yao, *J. Electroanal. Chem.*, 414 (1996) 53-59.
- [15] W. Haiss, J.K. Sass, *Langmuir*, 12 (1996) 4311-4313.
- [16] A. Hamelin, Double layer properties at sp and sd Metal Single-Crystal electrodes, in, Plenum, New York, 1985, pp. 1-101.
- [17] A. Hamelin, *J. Electroanal. Chem.*, 407 (1996) 13-21.
- [18] J. Lecoq, J. Andro, R. Parsons, *Surf. Sci.*, 114 (1982) 320-330.
- [19] J. Lecoq, J.P. Bellier, C. Koehler, *Electrochim. Acta*, 35 (1990) 1383-1392.
- [20] J. Lecoq, J.P. Bellier, C. Koehler, *J. Electroanal. Chem.*, 337 (1992) 197-216.
- [21] J. Lecoq, J.P. Bellier, C. Koehler, *J. Electroanal. Chem.*, 375 (1994) 117-122.
- [22] A. Hamelin, L. Stoicoviciu, F. Silva, *J. Electroanal. Chem.*, 229 (1987) 107-124.
- [23] A. Hamelin, L. Stoicoviciu, F. Silva, *J. Electroanal. Chem.*, 236 (1987) 283-294.
- [24] F. Silva, M.J. Sottomayor, A. Hamelin, L. Stoicoviciu, *J. Electroanal. Chem.*, 295 (1990) 301-316.
- [25] F. Silva, M.J. Sottomayor, A. Hamelin, *J. Electroanal. Chem.*, 294 (1990) 239-251.
- [26] F. Silva, M.J. Sottomayor, A. Martins, *J. Electroanal. Chem.*, 360 (1993) 199-210.
- [27] F. Silva, M.J. Sottomayor, A. Martins, *J. Chem. Soc., Faraday Trans.*, 92 (1996) 3693-3699.
- [28] S. Trasatti, The Electrode Potential, in, Plenum, New York, 1980, pp. 45-81.
- [29] S. Trasatti, *Electrochim. Acta*, 36 (1991) 1659-1667.
- [30] R.P. S. Trasatti, *J. Electroanal. Chem.*, 205 (1986) 359-376.
- [31] Z.F. Su, J. Leitch, J. Lipkowski, *Z Phys Chem*, 226 (2012) 995-1009.
- [32] T. Pajkossy, D.M. Kolb, *Electrochem. Commun.*, 5 (2003) 283-285.
- [33] T. Iwasita, X.H. Xia, *J. Electroanal. Chem.*, 411 (1996) 95-102.
- [34] V. Climent, B.A. Coles, R.G. Compton, *J. Phys. Chem. B*, 106 (2002) 5988-5996.
- [35] V. Climent, B.A. Coles, R.G. Compton, *J. Phys. Chem. B*, 106 (2002) 5258-5265.
- [36] V. Climent, B.A. Coles, R.G. Compton, J.M. Feliu, *J. Electroanal. Chem.*, 561 (2004) 157-165.
- [37] V. Climent, N. Garcia-Araez, R.G. Compton, J.M. Feliu, *J. Phys. Chem. B*, 110 (2006) 21092-21100.
- [38] N. Garcia-Araez, V. Climent, J.M. Feliu, *J. Am. Chem. Soc.*, 130 (2008) 3824-3833.
- [39] N. Garcia-Araez, V. Climent, J. Feliu, *J. Phys. Chem. C*, 113 (2009) 19913-19925.
- [40] N. Garcia-Araez, V. Climent, J. Feliu, *J. Phys. Chem. C*, 113 (2009) 9290-9304.
- [41] N. Garcia-Araez, V. Climent, J.M. Feliu, *Electrochim. Acta*, 54 (2009) 966-977.
- [42] I. Villegas, M.J. Weaver, *J. Phys. Chem. B*, 101 (1997) 10166-10177.
- [43] M.J. Weaver, *Langmuir*, 14 (1998) 3932-3936.
- [44] V. Climent, R. Gómez, J.M. Feliu, *Electrochim. Acta*, 45 (1999) 629-637.
- [45] A. Cuesta, *Surf. Sci.*, 572 (2004) 11-22.
- [46] M.J. Weaver, S.C. Chang, L.W.H. Leung, X. Jiang, M. Rubel, M. Szklarczyk, D. Zurawski, A. Wieckowski, *J. Electroanal. Chem.*, 327 (1992) 247-260.
- [47] N. Garcia-Araez, V. Climent, E. Herrero, J.M. Feliu, J. Lipkowski, *Electrochim. Acta*, 51 (2006) 3787-3793.
- [48] T. Pajkossy, D.M. Kolb, *Electrochim. Acta*, 46 (2001) 3063-3071.
- [49] E. Sibert, R. Faure, R. Durand, *J. Electroanal. Chem.*, 515 (2001) 71-81.
- [50] R. Gómez, V. Climent, J.M. Feliu, M.J. Weaver, *J. Phys. Chem. B*, 104 (2000) 597-605.
- [51] E. Morallon, J.L. Vazquez, A. Aldaz, *J. Electroanal. Chem.*, 288 (1990) 217-228.
- [52] R. Subbaraman, N. Danilovic, P.P. Lopes, D. Tripkovic, D. Strmcnik, V.R. Stamenkovic, N.M. Markovic, *J. Phys. Chem. c*, 116 (2012) 22231-22237.
- [53] M.J.S. Farias, C. Busó-Rogero, R. Gisbert, E. Herrero, J.M. Feliu, *J. Phys. Chem. c*, 118 (2013) 1925-1934.
- [54] J. Clavilier, D. Armand, S.G. Sun, M. Petit, *J. Electroanal. Chem.*, 205 (1986) 267-277.
- [55] V. Lazarescu, J. Clavilier, *Electrochim. Acta*, 44 (1998) 931-941.
- [56] O.A. Petrii, T.Y. Safonova, *J. Electroanal. Chem.*, 688 (2013) 336-348.
- [57] A. Berna, A. Rodes, J.M. Feliu, F. Illas, A. Gil, A. Clotet, J.M. Ricart, *J. Phys. Chem. B*, 108 (2004) 17928-17939.

- [58] Z.F. Su, V. Climent, J. Leitch, V. Zamlynyy, J.M. Feliu, J. Lipkowski, *Phys. Chem. Chem. Phys.*, 12 (2010) 15231-15239.
- [59] N. Garcia-Araez, V. Climent, P. Rodriguez, J.M. Feliu, *Langmuir*, 26 (2010) 12408-12417.
- [60] V. Buch, A. Milet, R. Vacha, P. Jungwirth, J.P. Devlin, *Proc. Natl. Acad. Sci. U. S. A.*, 104 (2007) 7342-7347.
- [61] R. Vacha, V. Buch, A. Milet, J.P. Devlin, P. Jungwirth, *Phys. Chem. Chem. Phys.*, 9 (2007) 4736-4747.

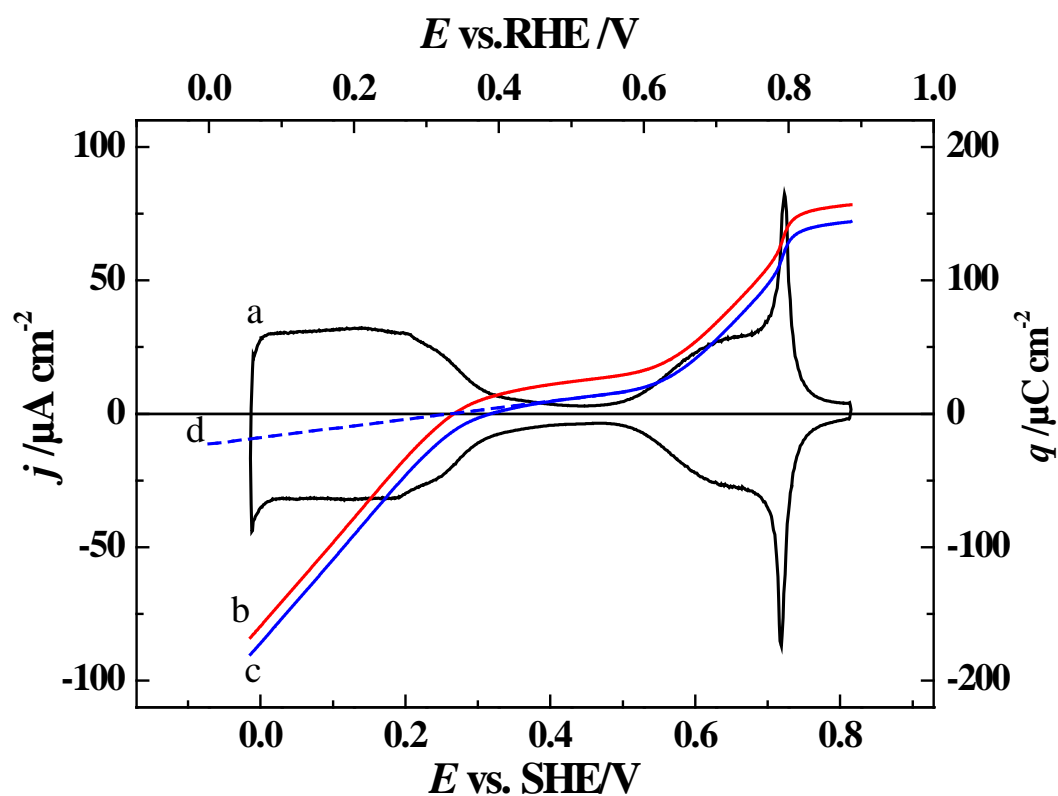


Figure 1: a) Cyclic voltammetry of Pt(111) in 0.1 M HClO_4 (pH=1,2) Sweep rate: 50 mV/s. b) Total charge density integrated from the voltammogram using equation **¡Error! No se encuentra el origen de la referencia.** in combination with the displaced charge at $E^*=0.1$ V. c) Corrected charge density taking into account the remaining charge on the CO covered surface, q_{CO} , calculated according to equation (2). d) Extrapolated charge density from the double layer region.

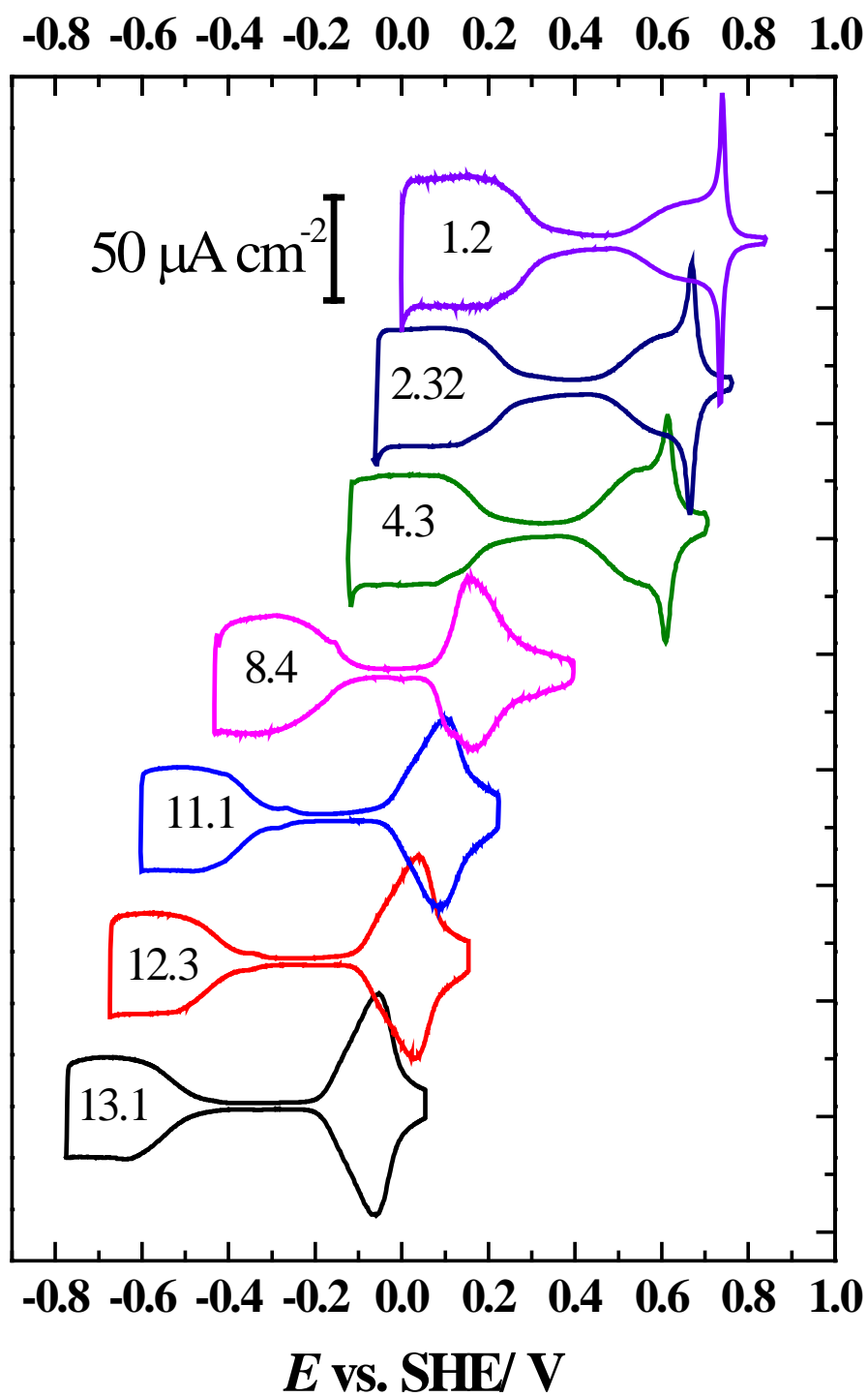


Figure 2. Cyclic voltammetry of the Pt(111) electrode in the different solutions employed. The number indicates the solution pH. For the solution compositions, see table 1. Scan rate: 50 mV s^{-1} .

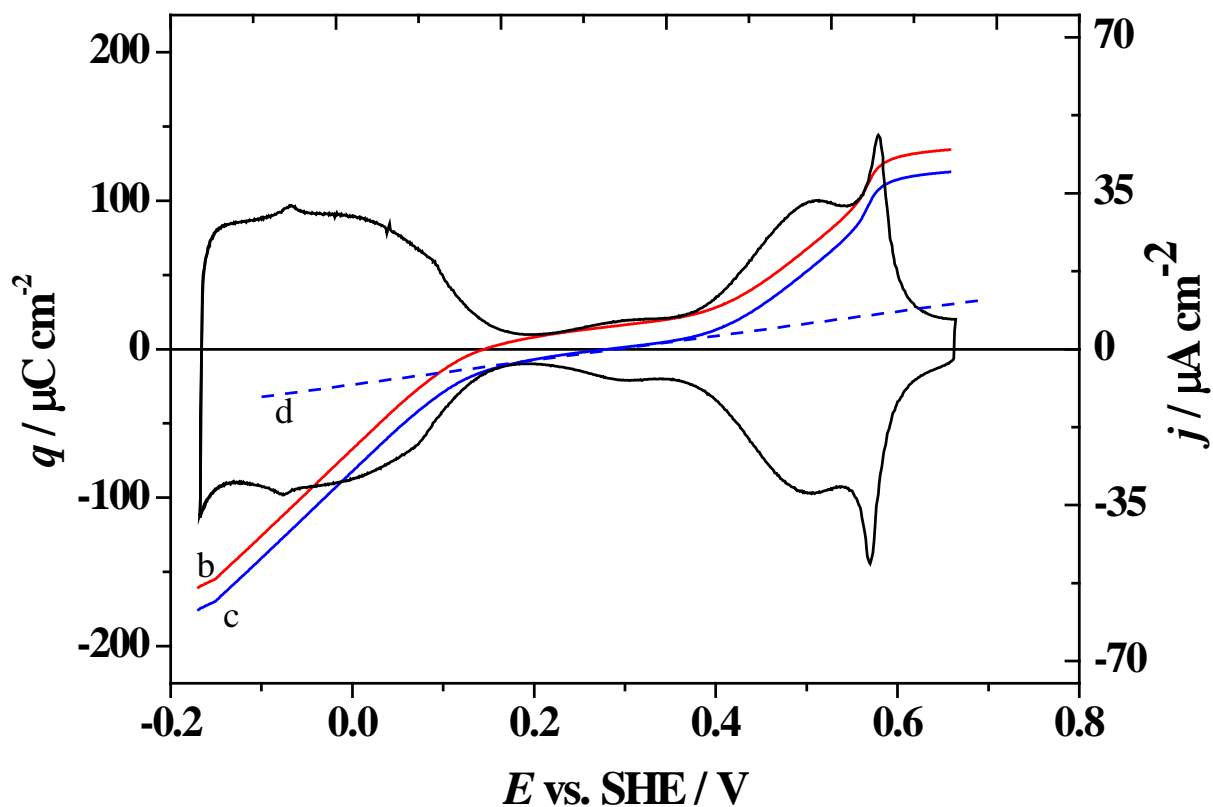


Figure 3: a) Cyclic voltammetry of Pt(111) in 0.099 M KClO_4 + 0.1 M HClO_4 (pH=3.4) Sweep rate: 50 mV/s. b) Total charge density integrated from the voltammogram using equation **¡Error! No se encuentra el origen de la referencia.** in combination with the displaced charge at $E^*=0.1$ V (RHE). c) Corrected charge density to take into account the remaining charge on the CO covered surface, q_{CO} . d) Extrapolated charge density from the double layer region

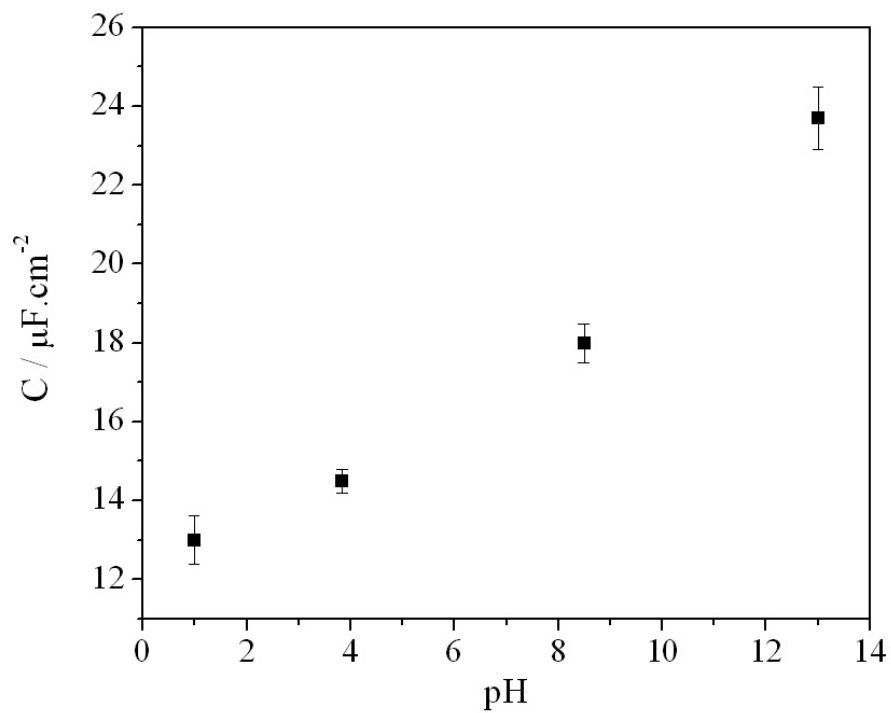


Figure 4. Measured double layer capacitances as a function of the solution pH for a CO covered Pt(111) dosed in acidic solutions.

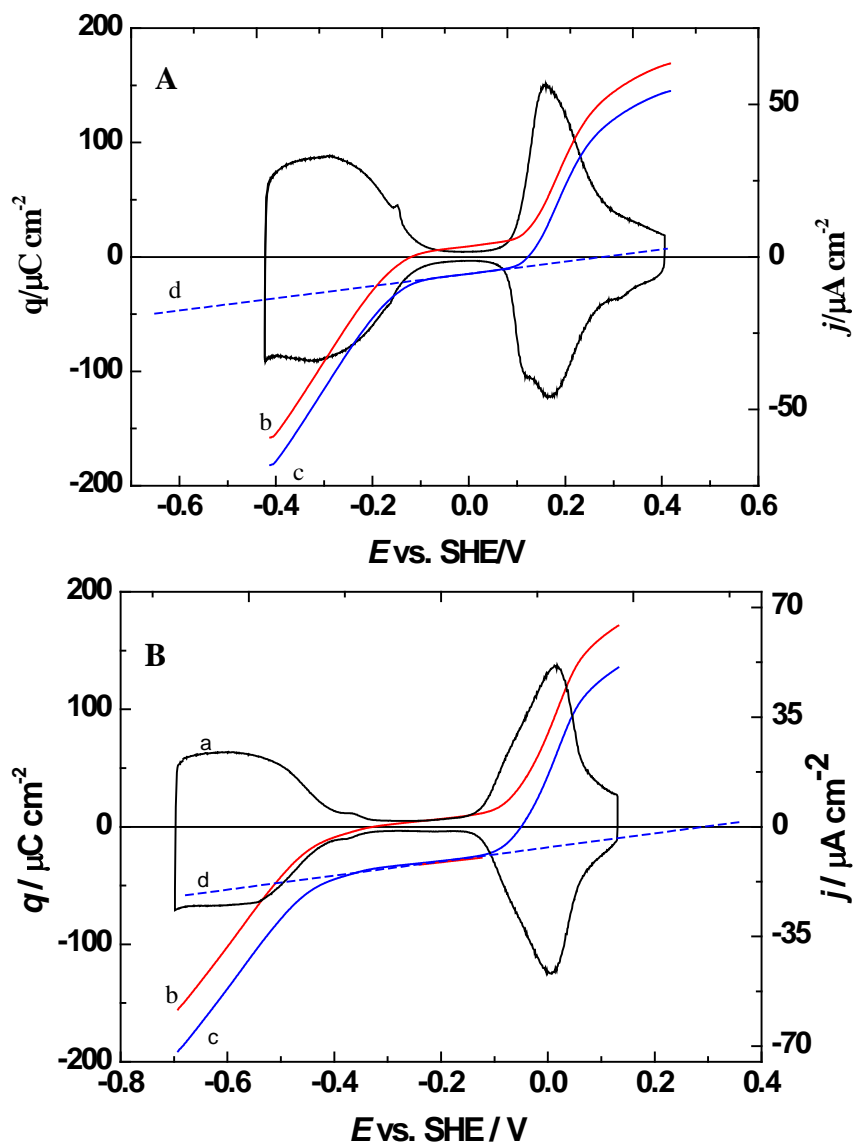


Figure 5: A) a) Cyclic voltammetry of Pt(111) in 0.1 M NaHCO_3 (pH=8.4) Sweep rate: 50 mV/s. b) Total charge density integrated from the voltammogram using equation **¡Error! No se encuentra el origen de la referencia.** in combination with the displaced charge at $E^*=0.1$ V (RHE). c) Corrected charge density to take into account the remaining charge on the CO covered surface, q_{CO} . d) Extrapolated charge density from the double layer region B) As in panel A but in 0.09 M KClO_4 +0.01 M NaOH

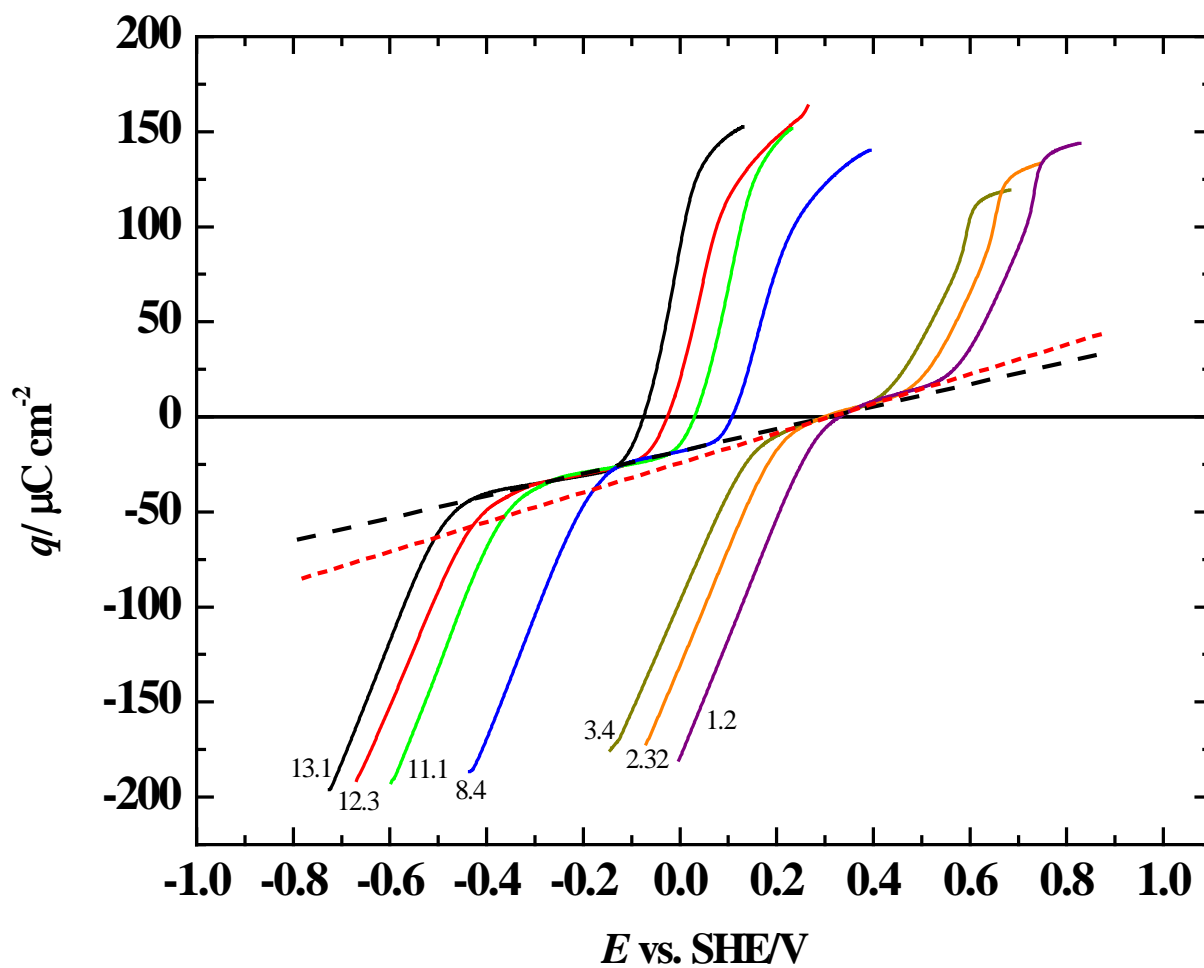


Figure 6. Corrected charge density curves measured at the different solutions for the Pt(111) electrode. The numbers indicate the solution pH. For the solution composition, see table 1. The dashed and dotted lines are the fittings in the double layer region of the charge density curves for the alkaline and acidic solutions, respectively.